

Strangeness production in proton-proton collisions ^{*†}

A. Sibirtsev and W. Cassing

Institut für Theoretische Physik, Universität Giessen
D-35392 Giessen, Germany,Institute of Physics, Jagellonian University
Reymonta 4, PL-30059 Cracow, Poland,Institute of Nuclear Physics
Radzikowskiego 152, PL-31342 Cracow, Poland

^{*}Supported by Forschungszentrum Jülich, the Jagellonian University of Cracow and the Cracow Institute of Nuclear Physics

[†]Seminars held at Institute of Physics, Jagellonian University.

Abstract

The cross sections of the reaction $pp \rightarrow NKY$ for K^+ or K^0 mesons and Λ or Σ hyperons are calculated within the boson exchange model including pion and kaon exchange diagrams. We analyze the dependence of the results on the accuracy of the input πN amplitude. By fixing the πNN coupling constant and the cut-off parameter Λ_π at the πNN vertex we calculate the contribution from the kaon exchange diagram and obtain the ratio of the $KN\Lambda$ and $KN\Sigma$ coupling constants by a fit to the experimental data. This ratio is in a good agreement with the $SU(6)$ prediction. Our calculated total cross sections for the different reaction channels are fitted by simple expressions and compared with other parameterizations used in the literature. Furthermore, the gross features of the production cross section close to threshold are discussed.

1 Introduction

The production of strange particles in nuclear collisions is an exciting subject in nuclear physics; e.g. strangeness enhancement is proposed as a signature for the formation of the quark gluon plasma in high energy nucleus-nucleus collision [1]. The production of strange particles in heavy-ion collisions at intermediate energies, furthermore, is also discussed as a way to study hot and dense nuclear matter [2, 3] due to the weak K^+N final state interaction.

During the last years K^+ meson production from heavy-ion collisions at energies per nucleon below the free NN reaction threshold was intensively studied at GSI [4], however, the interpretation of the experimental data is strongly model dependent because secondary production channels play a sensible role. Among the secondary reactions relevant for strangeness production at low energies are πN , ΔN and $\Delta\Delta$ collisions. As already discussed by Koch and Dover [5] the Δ might play an important role for subthreshold particle production. The heavy-ion simulations from Lang et al. [6], Huang et al. [7], Aichelin and Ko [8] and Li and Ko [9] show that the GSI data might be reproduced when accounting for the kaon production from the ΔN and $\Delta\Delta$ interactions. However, the former conclusion strongly depends upon the elementary $NN \rightarrow NYK$ cross section employed and the ratios between NN , ΔN and $\Delta\Delta$ reaction channels. More recent calculations on strangeness production in heavy-ion collisions [10], which are based on more reliable elementary cross sections [11], indicate that the $\pi N \rightarrow YK$ channels are dominant at low energies. Note, that the strangeness production via secondary meson-meson, meson-baryon and baryon-baryon interactions is also important for AGS energies [12]. Furthermore, experimental information on subthreshold strangeness production in $pA \rightarrow K^+X$ reactions is available from SATURNE [13] and CELSIUS [14] and will be available at COSY [15] soon.

The most important ingredients for the proton-nucleus and heavy-ion simulations are the elementary cross sections for strange particle production. From the experimental data we know the $\pi N \rightarrow KY$ amplitude rather well whereas the $BB \rightarrow BYK$ cross section is not well determined, since before 1997 the available experimental data on the reaction were very scarce [16]. A sizeable step forward was achieved recently with the measurement of the $pp \rightarrow p\Lambda K^+$ cross section by the COSY-11 Collaboration [17]. This reaction was studied very close to threshold and could clarify the validity of the old parameterizations on strangeness production from Randrup and Ko [18] and Zwermann and Schürmann [19], which have previously been used for $p + A$ and $A + A$ simulations.

However, inspite of the experimental progress our understanding of the reaction mechanism is still poor. The predictions of Li and Ko [20] and Sibirtsev [11] quite reasonably reproduce the data [16, 17] based on the K -meson exchange mechanism, while the study of Fäldt and Wilkin [21] and Tsushima et al. [22, 23, 24] indicate a dominance of π -meson exchange followed by the excitation of a $N^*(1650)$ baryonic resonance decaying to KY . In principle, by varying the model parameters both approaches can describe the experimental data. Thus the most constructive analysis of the present status is to investigate the model uncertainties as well as the selfconsistency of the calculations.

Recently, the most detailed analysis in the resonance model for strangeness pro-

duction was performed by Sibirtsev, Tsushima and Thomas [24]. Here the most crucial parameters entering the $pp \rightarrow p\Lambda K^+$ calculations are efficiently fixed by the $\pi N \rightarrow \Lambda K$ reaction [25] which clarifies the uncertainties of the resonance approach [21, 22]. Here we analyze the role of the kaon exchange mechanism for strangeness production and investigate to what extent our results might be influenced by the model parameters. Our study is organized as follows: In Section 2 we review the theoretical status and the uncertainties of the model while in Section 3 we formulate the one-meson exchange model. Our results from the calculations with pion and kaon exchange diagrams are discussed in Sections 4 and 5, respectively. In Section 6, furthermore, we analyze the near-threshold behavior of the total production cross section while a summary is presented in Section 7.

2 Theoretical status and uncertainties

The forces between baryons are traditionally considered as due to boson exchange. One of the models proposed to calculate the nucleon-nucleon scattering is the single pion exchange [26, 27]. An application of the meson exchange to photoproduction was performed already in 1961 by Sakurai [28], while for inelastic processes it was first investigated by Chew and Low [29]. A first application of the boson exchange mechanism to the calculation of strangeness production in proton-proton collisions at the energy of 3 GeV was performed in 1960 by Ferrari [30]. Here, pion and kaon exchange graphs were considered and it was found that the contribution from the pion exchange to the $pp \rightarrow p\Lambda K^+$ reaction cross section is about twice less than that from kaon exchange. The relevant diagrams for kaon production from pp collisions are shown in Figs. 1,2.

Within a similar approach, but neglecting the contribution from the kaon exchange diagram, Yao [31] calculated the strangeness production in the reactions $pp \rightarrow NYK$ and $pp \rightarrow NYK\pi$ at 2.9 GeV and rather well reproduced the total cross section as well as momentum and angular distributions. In his calculations it was assumed that the cut-off parameter of the pion form factor is given by the squared nucleon mass while the energy dependence of the $\pi N \rightarrow YK$ amplitude was neglected. Later on, Wu and Ko [32] calculated the energy dependence of the production cross section for the reaction $pp \rightarrow p\Lambda K^+$. Using only the one pion exchange they could reasonably well fit the available experimental data and thus pointed out a negligible contribution from the kaon exchange diagram.

A more detailed calculation of the associated strangeness production in proton-proton collisions was performed by Laget [33]. Within the boson exchange model it was found that the pion exchange accounts only for about 20% of the total $pp \rightarrow p\Lambda K^+$ cross section whereas the residual cross section is due to the kaon exchange mechanism. It was also shown that the dominant contribution to the cross section of the reaction $pp \rightarrow N\Sigma K$ stems from the one-pion exchange diagrams due to the small coupling constant $g_{N\Sigma K}^2 \simeq 0.8$.

The most surprising results were obtained by Deloff [34] within the pion and the kaon exchange model. He found that the experimental data can be reproduced by the pion and kaon exchange mechanism with the coupling constants $g_{N\Lambda K}^2 \ll g_{N\Sigma K}^2$ which strongly contradicted the previous calculations as well as the present understanding of the YN interaction [35, 36].

More recent calculations on $BB \rightarrow NYK$ reactions including proton, neutron and Δ -resonances in the entrance channel and accounting for both pion and kaon exchanges were performed by Li and Ko [20] using the coupling constants and cut-off parameters from Ref. [33]. Moreover, similar to Laget [33] both the $\pi N \rightarrow YK$ and $KN \rightarrow KN$ amplitudes were taken off-shell. The latter assumption is the basic difference between our calculations and those from Refs. [33, 20]. In our approach, to be described below, we will adopt on-shell amplitudes in the upper vertices in the diagrams presented in Figs. 1,2.

Calculations of the K -meson production in proton-proton collisions close to threshold within the one-pion exchange followed by $N^*(1650)$ resonance excitation were performed by Fäldt and Wilkin [21]. Actually the pion exchange diagrams from Fig. 2 can be reversed to the graph shown in Fig. 3. Moreover, within this resonance model one has to account for all baryonic resonances R coupling to $R \rightarrow YK$ as well as to $R \rightarrow \pi N$, $R \rightarrow \eta N$ and $R \rightarrow \rho N$ channels. Thus the resonance model allows to treat not only the pion exchange, but also the η and ρ -meson exchanges simultaneously. Since the $N^*(1650)$ is the lowest baryonic resonances, which can decay to the ΛK channel, its contribution is dominant at low collision energies. Since $N^*(1650)$ is not coupled to the Σ channel, one has to account for other baryonic resonances to calculate $pp \rightarrow N\Sigma K$ cross sections [22].

The next $N^*(1710)$ resonance coupled to the ΛK channel has a larger mass and can be excited in pp collisions at energies around 100 MeV above the $pp \rightarrow p\Lambda K^+$ reaction threshold. Note that the $N^*(1650)$ does not decay to the ΣK channel and for the $pp \rightarrow N\Sigma K$ reaction it is necessary to incorporate both the $N^*(1710)$ and $\Delta(1920)$ resonances. Since the $N^*(1650)$ strongly couples to the pion (60-80%) and only slightly to the η -meson (3-10%), the motivation of Fäldt and Wilkin [21] appeared quite reasonable. The actual question is the absolute value of their prediction for the $pp \rightarrow p\Lambda K^+$ cross section.

The $N^*(1650) \rightarrow N\pi$ and $N^*(1650) \rightarrow \Lambda K$ branching ratios are known experimentally [37] and therefore the corresponding coupling constants can be reasonably fixed on resonance. Note that by changing the couplings one can vary only the absolute magnitude of the $pp \rightarrow p\Lambda K^+$ cross section, but not its energy dependence. Thus, in principle, keeping these constants as free parameters one can perfectly reproduce the experimental data near threshold [17]. However, these parameters can be varied only within a certain range in line with the particle properties [37]. A more consistent calculation within the resonance model and for the $pp \rightarrow N\Lambda K$ and $pp \rightarrow N\Sigma K$ reactions was performed by Tsushima, Sibirtsev and Thomas [22, 24]. To avoid the uncertainties in the coupling constants and cut-off parameters the latter were taken from the analysis of the $\pi N \rightarrow \Lambda K$ and $\pi N \rightarrow \Sigma K$ reactions. Moreover, their calculations were performed for a wide range of pp collision energies in order to reproduce the recent near-threshold experimental data [17] as well as the results available at high energies [16]. All available and relevant baryonic resonances as well as π , η and ρ -meson exchanges were properly included. However, it was found that the calculations within the resonance model [22, 23] underestimate the $pp \rightarrow p\Lambda K^+$ cross section at low energy.

Let us now discuss the uncertainties of the calculations within the pion and kaon exchange model. Obviously, the calculations with the boson exchange model following the prescription from Figs.1,2 substantially depend on the accuracy of the

$\pi N \rightarrow YK$ and $KN \rightarrow KN$ amplitudes entering the calculations. Again, quite reliable studies for the $\pi N \rightarrow YK$ reaction within the resonance model were done by Tsushima, Huang and Faessler [25] who perfectly describe all channels of the $\pi N \rightarrow YK$ reaction at low energies. The $\pi N \rightarrow YK$ reaction was also investigated within the microscopic quark model by Yan, Huang and Faessler [38]. Moreover, the experimental data on strangeness production in pion induced reactions are well suited to perform simple parametrizations [39, 40] of the $\pi N \rightarrow YK$ cross sections and to adopt them for the $pp \rightarrow NYK$ calculations within the pion-exchange model.

On the other hand, the $KN \rightarrow KN$ amplitude cannot be well determined from the experimental data, since these are available for the $I = 1$ channel only, which corresponds to the reaction $K^+p \rightarrow K^+p$. The reconstruction of the $I = 0$ amplitude is not very accurate [41, 42], but this cross section is important for the kaon exchange model because it contributes to the following two-body amplitudes:

$$\begin{aligned} M(K^+p \rightarrow K^+p) &= M(K^0n \rightarrow K^0n) = M_1 \\ M(K^+n \rightarrow K^+n) &= M(K^0p \rightarrow K^0p) = \frac{1}{2} (M_0 + M_1) \\ M(K^+n \rightarrow K^0p) &= M(K^0p \rightarrow K^+n) = \frac{1}{2} (M_1 - M_0) \end{aligned} \quad (1)$$

A substantial progress in the calculation of the M_0 amplitude was achieved recently by the Jülich group [43] in analyzing KN elastic cross sections. On the other hand, to calculate the contribution from the kaon exchange to the $pp \rightarrow p\Lambda K^+$ cross section, one needs the $I = 1$ amplitude only. The coupling constants $g_{NN\pi}$, $g_{N\Lambda K}$ and $g_{N\Sigma K}$ as well as the corresponding cut-off parameters substantially influence the relative contribution from the pion and the kaon exchange mechanism. Actually we consider the coupling constant $g_{NN\pi}$ as well as the cut-off parameter Λ_π in the $NN\pi$ vertex to be fixed by the analysis in the Bonn model [44].

Furthermore, the $g_{N\Lambda K}$ and $g_{N\Sigma K}$ couplings are related to the mixing angle ϵ between the Λ and Σ contents of the nucleon as

$$\mathcal{R} = \frac{g_{K\Lambda\Lambda}^2}{g_{K\Lambda\Sigma}^2} = 3 \cot^2 \epsilon. \quad (2)$$

$SU(6)$ symmetry predicts $\epsilon = 18.4^\circ$ and thus a ratio $\mathcal{R} = g_{N\Lambda K}^2/g_{N\Sigma K}^2 \approx 27/1$. Note that when using the resonance prescription the coupling constant is related to the partial decay width of the resonance and thus the g_{NYK} coupling defines the strangeness content $N \rightarrow YK$ of the nucleon. This clearly indicates the importance of the $NN \rightarrow NYK$ reactions for the understanding of the fundamental properties of the nucleon.

In Table 1 we summarize the results on \mathcal{R} obtained from the KN dispersion relations [45, 46]. The coupling constants from Dalitz et al. [46] were obtained by an analysis of the total set of experimental data on KN scattering. The result from the meson exchange calculation of Laget [33] is close to the prediction from $SU(6)$ symmetry, while the ratio \mathcal{R} from Deloff [34] is the smallest value among those obtained presently. The result of Siebert et al. [47] was adjusted to the experimental data from SPES4 at SATURNE.

We note, that the interference due to the exchange of the nucleons for the s -wave phase shift, which is relevant for $K^+p \rightarrow K^+p$ elastic scattering at low energies,

Table 1: Cut-off parameters and coupling constants from different studies

Reference	Λ_K [GeV]	Λ_π [GeV]	$g_{N\Lambda K}^2$	$g_{N\Sigma K}^2$	\mathcal{R}
Martin [45]			13.9 ± 2.6	3.3 ± 1	4.2 ± 1.5
McGinley [46]			9.0	1.5	6
Dalitz [46]			20.7	1.0	20.7
Laget [33]	0.85	1.2	14	1	14
Deloff [34]					0.08
Siebert [47]					1.6
Our results	0.81 ± 0.14	1.0	19.6 ± 4.2	1.3 ± 0.3	15 ± 6
$SU(6)$					27

might change the model results by around 30% [48]. However, this interference is neglected in most of the calculations. Furthermore, the interference term between pion and kaon exchange substantially depends on the phase shifts of the $\pi N \rightarrow YK$ and $KN \rightarrow KN$ amplitudes. To fix the relative sign between the $\pi N \rightarrow YK$ and $KN \rightarrow KN$ exchange amplitudes one needs a well-defined interacting Lagrangian [20]. Alternatively, Laget proposed [33] to choose the sign in order to maximize the strangeness production cross section.

The analysis of the differential cross sections for the reaction $pp \rightarrow NYK$ were performed in Refs. [33, 34, 47] and contain much more uncertainties. To calculate the kaon as well as the baryon spectra one needs to incorporate the t -dependence of the $\pi N \rightarrow YK$ and $KN \rightarrow KN$ amplitudes. It is also discussed that the hyperon-nucleon interaction in the final state might change the observed spectra. In this sense the analysis of the total production cross section contains less uncertainties.

Actually there is no straightforward way to perform the calculations with such large uncertainties in the model parameters as the coupling constants, cut-offs as well as $\pi N \rightarrow YK$ and $KN \rightarrow KN$ amplitudes. Therefore, in order to proceed the calculation we propose the following scheme:

We assume that the coupling constant $g_{NN\pi}$ and the cut-off parameter Λ_π are fixed by the Bonn model [44] as well as an analysis of pion production from proton-proton collisions [44, 49] and first calculate the cross section of the reactions $pp \rightarrow p\Lambda K^+$ and $pp \rightarrow N\Sigma K$ using pion exchange, only. The difference between the experimental data and the one-pion exchange model calculations then is fitted by the kaon exchange mechanism in order to obtain the ratio \mathcal{R} and the cut-off parameter Λ_K neglecting the interference terms and assuming isotropy of the KN elastic cross section at energies near the kaon production threshold.

3 The one-boson exchange formalism

A detailed description of the one-boson exchange model is given by Ferrari and Selleri [26] and Berestetsky and Pomeranchuk [50]. Consider a physical reaction in which two initial particles with 4-momenta p_a and p_b transform into three particles,

$$p_a + p_b \rightarrow p_1 + p_2 + p_3 \quad (3)$$

with final 4-momenta p_1 , p_2 and p_3 . Fig. 4 illustrates the Feynmann diagram of the process.

Taking the particle a of spin 1/2 and the exchange of a single spineless boson m with mass μ , the amplitude for this reaction M is given within the pole approximation as

$$M = g_{a1m} F(t) \bar{u}(p_1) O u(p_a) \frac{1}{t - \mu^2} M_1, \quad (4)$$

where g_{a1m} is the coupling constant of the $(a \rightarrow 1 + m)$ vertex, $F(t)$ is the form factor of the proper vertex part, O is the operator (which is γ_5 or 1 according to the parity of the exchanged boson) and $t = (p_a - p_1)^2$ is the 4-momentum transfer squared. In Eq. 4 M_1 is the amplitude of the process $m + b \rightarrow 2 + 3$, which is related to the physical cross section as [52]

$$|M_1|^2 = 64 \pi^2 s_1 \frac{q_m}{q_2} \frac{d\sigma(m + b \rightarrow 2 + 3)}{d\Omega}, \quad (5)$$

where $s_1 = (p_2 + p_3)^2$ is the squared invariant mass of the (2+3) system, while q_m and q_2 are the momenta of the corresponding particles in the center-of-mass for this system. In this way one is allowed to introduce experimental information in the calculations within the boson exchange model.

The pole approximation implies that the formalism is valid within the limit $|t| \rightarrow \mu^2$ with μ being the mass of the exchanged particle. As was discussed in Ref. [50], at small values of the transferred momentum, $|t| \leq \mu^2$, the pole term (4) should yield the correct magnitude of the cross section (3) while at large $|t|$ one should take care about the corrections to the amplitude M .

Now the double differential cross section for the reaction (3) can be expressed as

$$\frac{d^2\sigma}{dt ds_1} = \frac{1}{2^9 \pi^3 q_a^2 s} \frac{q_2}{\sqrt{s_1}} |M|^2, \quad (6)$$

where $s = (p_a + p_b)^2$ is the squared invariant mass of the colliding particles and q_a is the momentum of particle a in their center-of-mass. Substituting the squared amplitude from Eq. 4 one can easily obtain the general expression

$$\frac{d^2\sigma}{dt ds_1} = \frac{g_{a1m}^2}{32\pi^2 q_a^2 s} q_m \sqrt{s_1} \frac{F^2(t)}{(t - \mu^2)^2} [(m_1 \pm m_a)^2 - t] \sigma(m + b \rightarrow 2 + 3), \quad (7)$$

where a plus sign has to be chosen if the exchanged meson is scalar and a minus sign if it is pseudoscalar [51]. The spin summation and averages of $|M|^2$ are assumed to be included and not written explicitly. Besides the form factor $F(t)$ Eq. 7 is the same as in Ref. [48] performed within the S -matrix approach.

The total cross section can now be obtained by integrating the expression (7) over the momentum transfer and the invariant mass of the (2+3) system. The ranges of integrations are given in Ref. [52].

A form factor is introduced in order to avoid the divergence of the total cross section at large collision energy or large momentum transfer. The sensitivity of the model results due to different types of form factors were studied in detail in the Jülich-Bonn potential model [43, 44, 54]. We note that one of the relevant historical methods is to cut the integration of Eq. 7 by a proper choice of the maximal value of $|t|$. Another well known method is to use a 'reggeized' boson exchange [53].

4 The pion exchange model

In our calculations we account for the one-pion exchange diagrams shown in Fig. 1. Within the pion exchange model the cross sections for the reactions $pp \rightarrow p\Lambda K^+$ and $pp \rightarrow N\Sigma K$ are given as

$$\sigma(pp \rightarrow NYK, \sqrt{s}) = \frac{m_N^2}{2\pi^2 q_i^2 s} \int_{W_{min}}^{W_{max}} k W^2 \sigma(\pi N \rightarrow KY, W) dW \times \int_{t_-}^{t_+} \frac{f_{NN\pi}^2}{\mu^2} F^2(t) D^2(t) t dt, \quad (8)$$

where \sqrt{s} and W are the invariant masses of the colliding protons and the produced kaon-hyperon system, respectively. Obviously we have

$$W_{min} = m_Y + m_K \quad \text{and} \quad W_{max} = \sqrt{s} - m_N \quad (9)$$

with m_N , m_Y and m_K being the masses of the nucleon, Λ or Σ -hyperon and K -meson, respectively. In Eq. (8) t stands for the squared four-momentum transfer from the initial to the final nucleon and

$$t_{\pm} = 2m_N^2 - 2E_i E_f \pm 2q_i q_f, \quad (10)$$

where E_i , q_i are the energy and the momentum of the initial nucleons in the center-of-mass frame, while E_f , q_f are that for the final nucleons; μ and k denote the mass and momentum of the exchange pion. With the kinematical function

$$\lambda(x, y, z) = (x - y - z)^2 - 4yz \quad (11)$$

one can simply express the momenta as

$$\begin{aligned} q_i^2 &= \lambda(s, m_N^2, m_N^2)/4s \\ q_f^2 &= \lambda(s, W^2, m_N^2)/4s \\ k^2 &= \lambda(W^2, m_N^2, \mu^2)/4W^2. \end{aligned} \quad (12)$$

The pion propagator is given by

$$D(t) = \frac{1}{t - \mu^2}; \quad (13)$$

the coupling constant $f_{NN\pi}^2 = 1.0$ is similar to that used in Refs. [55, 33, 56, 20]. Note, that the renormalized coupling constant $f_{NN\pi}$ is related to $g_{NN\pi}$ as [50]

$$\frac{f^2}{4\pi} = \frac{g^2}{4\pi} \left(\frac{\mu}{2m_N} \right)^2 \quad (14)$$

with $g^2/4\pi = 14.4$ [44]. To account for the off-shell modification of the $NN\pi$ vertex we use a monopole form factor

$$F(t) = \frac{\Lambda_\pi^2 - \mu^2}{\Lambda_\pi^2 - t} \quad (15)$$

with the pion cut-off parameter $\Lambda_\pi = 1$ GeV. Furthermore, $\sigma(\pi N \rightarrow KY, W)$ is the cross section for the corresponding $\pi p \rightarrow KY$ channel. Isospin symmetry is applied in order to get the relations between the different channels with Λ and Σ hyperon production, i.e.

$$\begin{aligned}\sigma(\pi^0 p \rightarrow K^+ \Lambda) &= \frac{1}{2} \sigma(\pi^- p \rightarrow K^0 \Lambda) \\ \sigma(\pi^0 p \rightarrow K^0 \Sigma^+) &= \sigma(\pi^+ n \rightarrow K^+ \Sigma^0).\end{aligned}\quad (16)$$

As already discussed in Section 2 the $\pi N \rightarrow KY$ cross section may be taken either from the calculations within the resonance model [25] or in form of a parameterization of the relevant experimental data [39].

Let us to remind that the difference of the present model prescription of the $pp \rightarrow NYK$ reaction to that proposed by Li and Ko [20] is due to the introduction of the form factor (15) in the upper πNYK vertex of the diagrams in Fig. 1 accounting for the off-shell nature of the exchanged pion. This correction was included in the calculations [20] and thus the results from [20] should actually be lower than our calculations. We do not correct the $\pi N \rightarrow YK$ amplitude since in the calculations within the resonance model [25] the corresponding form factor was already introduced. Thus using the parameterization from [25] we effectively already account for the proper cross section.

The cross sections for the different channels of the reaction $\pi N \rightarrow YK$ can be parameterized as [25]

$$\sigma(\pi N \rightarrow KY) = \sum_j \frac{A_j(\sqrt{s} - \sqrt{s_{th}})^{f_j}}{(\sqrt{s} - M_j)^2 + B_j^2}, \quad (17)$$

where \sqrt{s} is the invariant mass of the πN system, $\sqrt{s_{th}} = m_K + m_Y$ was taken to be equal 1.613 GeV for ΛK and 1.688 GeV for ΣK production. The parameters A_j , f_j , M_j and B_j are listed in Table 2 for the relevant reaction channels.

Table 2: Parameters of the approximation (17).

Reaction	j	A [μb]	f	M [GeV]	B [MeV]
$\pi^- p \rightarrow K^0 \Lambda$	1	7.665	0.1341	1.72	88.465
$\pi^+ p \rightarrow K^+ \Sigma^+$	1	35.91	0.9541	1.89	124.418
$\pi^+ p \rightarrow K^+ \Sigma^+$	2	159.4	0.01056	3.0	970.155
$\pi^+ n \rightarrow K^+ \Sigma^0$	1	50.14	1.2878	1.73	80.343
$\pi^0 p \rightarrow K^+ \Sigma^0$	1	3.978	0.5848	1.74	81.67
$\pi^0 p \rightarrow K^+ \Sigma^0$	2	47.09	2.165	1.905	79.737

In order to study the sensitivity of the results within the pion exchange model on the accuracy of the incorporated πN amplitude we also test the reaction $pp \rightarrow p\Lambda K^+$ with two other parameterizations from Cugnon et al. [39, 40], i.e.:

$$\begin{aligned}\sigma(\pi^- p \rightarrow K^0 \Lambda) &= 9.8(\sqrt{s} - 1.6) \text{ at } \sqrt{s} < 1.7 \text{ GeV} \\ &= 0.084(\sqrt{s} - 1.6)^{-1} \text{ at } \sqrt{s} \geq 1.7 \text{ GeV}\end{aligned}\quad (18)$$

where the cross section is given in mb and

$$\begin{aligned}\sigma(\pi^- p \rightarrow K^0 \Lambda) &= 0.65p^{4.2} \text{ at } 0.9 < p < 1.0 \\ &= 0.65p^{-1.67} \text{ at } p \geq 1\end{aligned}\quad (19)$$

with the cross section given again in mb and the incident pion momentum in the laboratory frame p taken in GeV/c .

Fig. 5 shows the experimental cross section of the reaction $\pi^- p \rightarrow K^0 \Lambda$ from Ref. [16] together with the parameterizations (17) and (18). We stress the difference between the parameterizations at $\sqrt{s} > 2 \text{ GeV}$ which influences the results from the pion exchange model at large collision energies. However, in the maximum of the $\pi^- p \rightarrow K^0 \Lambda$ cross section the difference between (17) and (18) is only about 30%. The dotted line in Fig. 5 indicates the parameterization (19).

The resulting cross section for the reaction $pp \rightarrow p\Lambda K^+$ within the one-pion exchange model for different parameterizations of $\sigma(\pi^0 p \rightarrow K^+ \Lambda)$ together with the experimental data [16] are shown in Fig. 6 as a function of the proton beam energy. The notations are similar to those in Fig. 5.

We conclude that, i) the results from the pion exchange calculations with all different $\pi N \rightarrow \Lambda K$ parameterizations underestimate the experimental data for the reaction $pp \rightarrow p\Lambda K^+$ by a factor of 3. This discrepancy indicates the importance of the kaon exchange mechanism; ii) we find that the results strongly depend on the input $\pi N \rightarrow K\Lambda$ amplitude at high energies. Indeed, this was expected since calculations from Ref. [25] did not reproduce the $\pi N \rightarrow \Lambda K$ cross section at high energies (cf. Fig. 5). On the other hand, at low energies there are no differences between the results obtained with different $\pi N \rightarrow \Lambda K$ parameterizations. Moreover, the accuracy of the experimental data for pp collisions is better than the differences from the different $\pi N \rightarrow \Lambda K$ parameterizations. In the following calculations we thus use (17).

Within the one-pion exchange model we now also calculate the cross sections for the reactions $pp \rightarrow p\Sigma^+ K^0$, $pp \rightarrow p\Sigma^0 K^+$ and $pp \rightarrow n\Sigma^+ K^+$ involving a Σ in the final channel. Our model results are shown in Figs. 7,8 together with the experimental data. The calculations quite reasonably reproduce the data in case of $K\Sigma$ production and show not much room for the contribution from the kaon exchange graph.

5 The kaon exchange model

The kaon exchange diagrams are shown in Fig. 2 and the relevant cross sections are similar to (8)

$$\begin{aligned}\sigma(pp \rightarrow NYK, \sqrt{s}) &= \frac{m_N m_Y}{2\pi^2 p_i^2 s} \int_{W_{min}}^{W_{max}} k W^2 \sigma(KN \rightarrow KN, W) dW \times \\ &\quad \int_{t_-}^{t_+} \frac{f_{NYK}^2}{m_K^2} F^2(t) D^2(t) t dt,\end{aligned}\quad (20)$$

where m_Y is the mass of the produced hyperon (Λ or Σ) and W is the invariant mass of the kaon-nucleon system with

$$W_{min} = m_N + m_K, \quad W_{max} = \sqrt{s} - m_Y. \quad (21)$$

Here t is the squared four-momentum transfer from the initial proton to the hyperon and

$$t_{\pm} = m_N^2 + m_Y^2 - 2E_i E_Y \pm 2q_i q_Y, \quad (22)$$

where E_i, q_i are the same as in (8), while E_Y, q_Y are the energy and three-momentum of the hyperon in the center-of-mass frame. Note that k in this case denotes the momentum of the exchange kaon,

$$\begin{aligned} k^2 &= \lambda(W^2, m_N^2, m_K^2)/4W^2 \\ q_Y^2 &= \lambda(s, W^2, m_Y^2)/4s. \end{aligned} \quad (23)$$

In Eq. 20 $\sigma(KN \rightarrow KN, W)$ is the cross section for the $KN \rightarrow KN$ reaction. For $K^+p \rightarrow K^+p$ elastic scattering we adopt the parametrization from Cugnon et al. [40]

$$\sigma(K^+p \rightarrow K^+p) = 3 + 11.5 \left[1 + \exp \left(\frac{p - 1.06}{0.8} \right) \right]^{-1} \quad (24)$$

with the cross section given in mb and the laboratory kaon momentum p in GeV/c . Other $KN \rightarrow KN$ reaction channels - relevant for Σ -hyperon production (cf. Fig. 2) - were taken from Ref. [57]; the latter are not crucial since the coupling in the $N\Sigma K$ vertex is small.

The kaon propagator was taken similar to the pion replacing the π -meson mass by the kaon mass. We use the kaon form factor

$$F(t) = \frac{\Lambda_K^2 - \mu^2}{\Lambda_K^2 - t} \quad (25)$$

with a cut-off parameter Λ_K that has to be determined in comparison to the experimental data. The coupling constant $f_{N\Lambda K}^2$ has to be fitted by the difference between the experimental cross section for the reaction $pp \rightarrow p\Lambda K^+$ and the results from the pion exchange model. In a similar way we get $f_{N\Sigma K}^2$ using the $pp \rightarrow p\Sigma K$ reaction channels. The fitting procedure leads to the following parameters for the kaon exchange model

$$\Lambda_K = 0.81 \pm 0.14 \text{ GeV}, \quad f_{N\Lambda K}^2 = 14.6 \pm 3.1, \quad f_{N\Sigma K}^2 = 0.88 \pm 0.26. \quad (26)$$

The relation between f_{NYK} and g_{NYK} coupling constants is

$$\frac{f^2}{4\pi} = \frac{g^2}{4\pi} \frac{\mu^2}{4m_N m_Y} \quad (27)$$

where μ is the kaon mass and m_Y is the mass of the Λ or Σ -hyperon. Therefore the ratio of the $g_{N\Lambda K}$ and $g_{N\Sigma K}$ coupling constant equals to 15 ± 6 , which is in reasonable agreement with the $SU(6)$ prediction.

In Fig. 9 we display the contribution from the kaon exchange graph to the $pp \rightarrow p\Lambda K^+$ cross sections (dashed line) and the results obtained with the pion exchange model (dotted line). The sum of both contributions is shown by the solid line and perfectly describes the data at high as well as low energies.

Fig. 7 show the results calculated for the Σ -hyperon production. Unfortunately, the small number of the experimental points and large experimental errors substantially spoil the analysis.

6 Near-threshold behavior of the cross section

We note that different theoretical models [11, 20, 21, 22] predict a very similar energy dependence of the $pp \rightarrow p\Lambda K^+$ cross section close to the reaction threshold, i.e. at excess energies $\epsilon = \sqrt{s} - m_N - m_\Lambda - m_K \leq 100$ MeV. Moreover, this energy dependence reflects essentially the phase space of the production cross section which is expressed through Eq. (6) by using a constant amplitude for the reaction as

$$\sigma = \frac{R_3}{I} |M|^2 \quad (28)$$

with R_3 denoting the three-body phase space integral

$$R_3 = \frac{\pi^2}{4s} \int_{(m_\Lambda+m_K)^2}^{(\sqrt{s}-m_N)^2} \lambda^{1/2}(s, s_1, m_N^2) \lambda^{1/2}(s_1, m_\Lambda^2, m_K^2) \frac{ds_1}{s_1}, \quad (29)$$

while I is the flux factor [52]

$$I = 2 (2\pi)^5 \lambda^{1/2}(s, m_N^2, m_N^2). \quad (30)$$

The cross section calculated with constant amplitude is shown in Fig. 10 together with the experimental data [16, 17] as a function of the excess energy. Here we fit $|M|^2$ in order to match the experimental point from Ref. [17].

Let us now discuss why both our calculations and the results from the resonance model follow the phase space consideration. This similarity can be explained by the kinematical constraints of the reaction at low ϵ . Note that in any of the models the integration of the general expression (i.e. Eq. (6)) has to be performed over the variables t and s_1 , which depend only on the collision energy as well as on the mass of the final particle. For a fixed value of the excess energy ϵ the limits of the integration over s_1 are defined by

$$m_\Lambda + m_K \leq \sqrt{s_1} \leq m_\Lambda + m_K + \epsilon \quad (31)$$

for the pion exchange and

$$m_N + m_K \leq \sqrt{s_1} \leq m_N + m_K + \epsilon \quad (32)$$

for the kaon exchange. Thus the range of the integration is equal to the excess energy independent from the production mechanism. The relevant amplitude M_1 of the corresponding subprocess (as well as cross section) is almost energy independent for $\epsilon \leq 100$ MeV. Moreover, some of the earlier calculations on strangeness production [31, 48] simply neglect this energy dependence of the $|M_1|$ amplitude even for higher excess energies.

At low ϵ the t -dependence seems to be more crucial. However, at the reaction threshold $\sqrt{s} = m_N + m_\Lambda + m_K$ the momenta of the produced particles in the center-of-mass of the colliding nucleons are close to zero and the momentum transfer is determined as

$$t = 2m_N^2 - m_N \sqrt{s} = m_N(m_N - m_\Lambda - m_K) \simeq -0.63 \text{ GeV}^2. \quad (33)$$

Furthermore, lets look at the dependence of the momentum transfer on the collision energy. Fig. 11 shows the lower and upper limits of $-t$ as a function of the

available energy ϵ above the reaction threshold. Since the momentum transfer also depends on the invariant mass of the particle in the upper vertices of the diagrams shown in Figs. 1,2, we vary $\sqrt{s_1}$ within the range ϵ and display only the minimal and maximal values. Note that within the range $\sqrt{s} - \sqrt{s_0} < 100$ MeV t changes only slightly and is almost constant.

Thus the form factor and the propagator part of the reaction amplitude are almost constant as well as the amplitude itself. Consequently the production cross section at low ϵ follows the phase space dependence according to Eq. (28). Moreover, this property is fundamental for most of the reactions with particle production near threshold.

Apart from the latter considerations there are several factors which might change the energy dependence of the cross section relative to that from phase space. Most effective are interactions in the initial and final states. Following the effective range approximation one can assume that these interactions depend on the relative momentum of the particles. Particularly for strangeness production from pp collisions the relative momentum of the colliding nucleons is quite large in the initial state and their interaction here is suppressed. This is not the case for the final state where the strong hyperon-nucleon interaction can affect the total cross section close to threshold.

Fig. 10 shows the near-threshold behavior of the $pp \rightarrow p\Lambda K^+$ cross section calculated with our model and with the parameters fitted by the experimental data at higher energies. Our results reasonably describe the experimental point from COSY at $\epsilon = 2$ MeV [17]

7 Comparison with other pp parameterizations

The calculated cross sections for the reaction $pp \rightarrow NYK$ can be parameterized as

$$\sigma(pp \rightarrow NYK, \sqrt{s}) = a \left(1 - \frac{s_0}{s}\right)^b \left(\frac{s_0}{s}\right)^c \quad (34)$$

with $s_0 = 6.487$ GeV 2 for Λ and 6.864 GeV 2 for Σ production. The parameters a , b and c are obtained by fitting the results from the boson exchange model taking into account the contribution from both pion and kaon exchanges. In Table 3 we show the parameters for the different reaction channels.

Table 3: Parameters of the approximation (34).

Reaction	a [μb]	b	c
$pp \rightarrow p\Lambda K^+$	732.16	1.8	1.5
$pp \rightarrow p\Sigma^+ K^0$	338.46	2.25	1.35
$pp \rightarrow p\Sigma^0 K^+$	275.27	1.98	1.0
$pp \rightarrow n\Sigma^+ K^+$	549.51	1.87	0.98

Our parameterization for the reaction $pp \rightarrow p\Lambda K^+$ is shown in Fig. 12 together with the results from the boson exchange model and the experimental data. The

dashed line shows the parameterization proposed by Randrup and Ko [18]

$$\sigma(pp \rightarrow p\Lambda K^+) = 24 \frac{p_{max}}{m_K} \quad [\mu b] \quad (35)$$

with p_{max} given by

$$p_{max}^2 = \lambda(s, [m_N + m_\Lambda]^2, m_K^2)/4s. \quad (36)$$

The dotted line in Fig. 12 indicates the parameterization from Schürmann and Zwermann [19]

$$\sigma(pp \rightarrow K^+ X) = 31.7 \left(\frac{p_{max}}{m_K} \right)^4 \quad [\mu b]. \quad (37)$$

Since the parameterization [19] reflects the phase space energy dependence of the production cross section it is close to the results obtained with the boson exchange model.

The cross section for the reaction channels with a Σ hyperon is parameterized in [18] as

$$\sigma(pp \rightarrow p\Sigma^0 K^+) + \sigma(pp \rightarrow p\Sigma^+ K^0) = 24 \frac{p_{max}}{m_K} \quad [\mu b] \quad (38)$$

with the maximal kaon momentum p_{max} for the $N\Sigma K$ channel

$$p_{max}^2 = \lambda(s, (m_N + m_\Sigma)^2, m_K^2). \quad (39)$$

In Fig. 13 we show (38) together with our result. The cross section calculated within the boson exchange model is substantially smaller than the parameterization from Ref. [18].

The cross section for the inclusive K^+ -meson production from pp collisions is shown in Fig. 14 as a function of the bombarding energy. The squares show the experimental data for the reaction $pp \rightarrow p\Lambda K^+$ while the dotted line is our parameterization (34) for this channel. The dots are the experimental cross section for the inclusive reaction $pp \rightarrow K^+ X$. The dashed line shows the contribution from $pp \rightarrow N\Sigma K^+$ while the solid line is the sum of the Λ and Σ channels. Note that at incident proton energies above 2.5 GeV the contributions from the Σ reaction channels become larger than those from the Λ channel, which should be important for transport simulations of the K^+ production. At bombarding energies above 3.5 GeV the calculated cross section of the reaction $pp \rightarrow NYK^+$ underestimates the experimental data for inclusive kaon production substantially which demonstrates the importance of final channels with additional π -mesons.

8 Summary

Within the boson exchange model we have calculated the cross section for the reactions $pp \rightarrow NYK$ with a Λ , Σ -hyperon and K^0 , K^+ -meson. The contributions from the one-pion and kaon exchange were studied separately. We find that the dominant contribution to the reaction $pp \rightarrow p\Lambda K^+$ stems from the kaon exchange diagram, whereas Σ -hyperon production is dominated by one-pion exchange. The boson exchange model rather well describes the available experimental data on the reaction $pp \rightarrow NYK$. Furthermore, the ratio of the $N\Lambda K$ and $N\Sigma K$ coupling constants fitted to the experimental data is in good agreement with the $SU(6)$ prediction.

The near-threshold behavior of the production cross section was analyzed and shown to be dominated by phase space. The calculated cross sections were parameterized and compared with other parameterizations that have been widely used in proton-nucleus and heavy-ion simulations before.

It is found that the $pp \rightarrow N\Sigma K^+$ reaction dominates over Λ -hyperon production with increasing beam energy. The inclusive K^+ -meson production is described by the sum of the three body final state channels up to the incident proton energy of 3.5 GeV. At higher energies additional π -mesons in the final channel have to be taken into account.

The authors gratefully acknowledge stimulating discussions with L. Jarczyk, B. Kamys, C.M. Ko, U. Mosel, Z. Rudy, A. Strzalkowski and K. Tsushima. Furthermore, the authors like to thank the Institute of Physics at the Jagellonian University of Cracow for warm hospitality during their research visits.

References

- [1] J. Rafelski and B Müller, Phys. Rev. Lett. 48 (1982) 1066.
- [2] G.E. Brown, C.M. Ko, Z.G. Wu and L.H. Xia, Phys. Rev. C 43 (1991) 1881.
- [3] W. Cassing, V. Metag, U. Mosel and K. Niita, Phys. Rep. 188 (1990) 363.
- [4] W. Ahner, P. Baltes, R. Barth et al., GSI Scientific Report (1994) 38; P. Senger and the KaoS Collaboration, Acta Phys. Polonica B 27 (1996) 2993; R. Elmer, M. Berg, L. Carlén, B. Jakobsson et al., Phys. Rev. Lett. 77 (1997) 4884; R. Barth, P. Senger, W. Ahner, P. Beckerle et al., Phys. Rev. Lett. 78 (1997) 4007.
- [5] P. Koch and C. Dover, Phys. Rev. C 40 (1989) 145.
- [6] A. Lang, W. Cassing, U. Mosel and K. Weber, Nucl. Phys. A 541 (1992) 507.
- [7] S.W. Huang, A. Faessler, G.Q. Li, R.K. Puri and E. Lehmann, Phys. Lett. B 298 (1993) 41.
- [8] J. Aichelin and C.M. Ko, Phys. Rev. Lett. 55 (1985) 2661.
- [9] G.Q. Li and C.M. Ko, Phys. Lett. B 349 (1995) 405.
- [10] W. Cassing, E.L. Bratkovskaya, U. Mosel, S. Teis and A. Sibirtsev, Nucl. Phys. A 614 (1997) 415; E.L. Bratkovskaya, W. Cassing and U. Mosel, Nucl. Phys. A 622 (1997) 593.
- [11] A.A. Sibirtsev, Phys. Lett. B 359 (1995) 29.
- [12] J. Stachel, Nucl. Phys. A 527 (1991) 167.
- [13] M. Debowski et al., Z. Phys. A 356 (1996) 313.
- [14] A.Badala et al, *Proceedings of the International Conference on the Applications of Accelerators in Research and Industry*, Denton November 1996, J.L.Duggan and J.L.Morgan Eds., CP392 (1997) 357.
- [15] O.W.B. Schult et al., Nucl. Phys. A 583 (1995) 629.
- [16] A. Baldini, V. Flaminio, W.G. Moorhead and D.R.O. Morrison, *Landolt-Börnstein, Numerical Data and Functional Relationships in Science and Technology* vol. 12, ed. by H. Schopper, Springer-Verlag (1988).
- [17] J.T. Balewski et al., Phys. Lett. B 338 (1996) 859.
- [18] J. Randrup and C.M. Ko., Nucl. Phys. A 343 (1980) 519; Nucl. Phys. A 411 (1983) 537.
- [19] B. Schürmann and W. Zwermann, Phys. Lett. B 183 (1987) 31.
- [20] G.Q. Li and C.M. Ko, Nucl. Phys. A594 (1995) 439.
- [21] G. Fäldt and C. Wilkin, Z. Phys. A 357 (1997) 241.

- [22] K. Tsushima, A. Sibirtsev and A. W. Thomas, Phys. Lett. B 390 (1997) 29.
- [23] A. Sibirtsev, K. Tsushima and A. W. Thomas, sub. to Phys. Lett.; nucl-th/9711028
- [24] A. Sibirtsev, K. Tsushima and A. W. Thomas, sub. to Nucl. Phys.
- [25] K. Tsushima, S.W. Huang and Amand Faessler, Phys. Lett. B 337 (1994) 245; J. Phys. G 21 (1995) 33; Australian. J. Phys. 50 (1997) 35.
- [26] E. Ferrari and F. Selleri, Suppl. Nuovo Cim. 26 (1962) 451.
- [27] M.M. McGregor, M.J. Moravcsik and H.P. Stapp, Phys. Rev. 116 (1959) 1248; L.B. Okun and I.Ya. Pomeranchuk, Nucl. Phys. 10 (1959) 492; P.S. Signell, Phys. Rev. Lett. 5 (1960) 474.
- [28] J.J. Sakurai, Nuovo Cim. 20 (1961) 1212.
- [29] G.F. Chew and F.E. Low, Phys. Rev. 113 (1959) 1640.
- [30] E. Ferrari, Nuovo Cim. 15 (1960) 652.
- [31] T. Yao, Phys. Rev. 125 (1962) 1048.
- [32] J.Q. Wu and C.M. Ko, Nucl. Phys. A 499 (1989) 810.
- [33] J.M. Laget, Phys. Lett. B 259 (1991) 24.
- [34] A. Deloff, Nucl. Phys. A 505 (1989) 583.
- [35] P.M.M. Maessen, T.A. Rijken and J.J. de Swart, Phys. Rev. C 40 (1989) 2226.
- [36] A. Reuber, K. Holinde and J. Speth, Nucl. Phys. A 570 (1994) 543.
- [37] Particle Data Group, Phys. Rev. D 50 (1994).
- [38] Y. Yan, S.W. Huang and Amand Faessler, Phys. Lett. B 354 (1995) 24.
- [39] J. Cugnon and R.M. Lombard, Nucl. Phys. A 422 (1984) 635.
- [40] J. Cugnon, P. Deneye, P., Vandermeulen, J.: Phys. Rev. C 41 (1990) 1701.
- [41] B.R. Martin, Nucl. Phys. B 94 (1975) 413.
- [42] G. Giacomelli, Prog. Nucl. Phys. 12 (1970) 77.
- [43] M. Hoffmann, J.W. Durso, K. Holinde, B.C. Pearce and J. Speth, Nucl. Phys. A 593 (1995) 341.
- [44] R. Machleidt, K. Holinde, and C. Elster, Phys. Rep. 149 (1987) 1; R. Machleidt, Adv. Nucl. Phys. 19 (1989) 189.
- [45] A.D. Martin, Nucl. Phys. B 179 (1981) 33.

- [46] R.H. Dalitz, J. McGinley, C. Belyea and S. Anthony, *Proc. Int. Conf. on hypernuclear and kaon physics* Heidelberg (1982) ed. B.Povh.
- [47] R. Siebert et al., Nucl. Phys. A 567 (1994) 819.
- [48] E. Ferrari, Phys. Rev. 120 (1960) 988.
- [49] K.G. Boreskov, A.B. Kaidalov and V.I. Lisin, Sov. J. Nucl. Phys. 15 (1972) 203.
- [50] V.B. Berestetsky and I. Ya. Pomeranchuk, Nucl. Phys. 22 (1961) 629.
- [51] J.D. Bjorken and S.D. Drell, *Relativistic Quantum Mechanics* McGraw-Hill Book Co. (1964)
- [52] E. Byckling and K. Kajantie, *Particle Kinematics* John Wiley and Sons (1973).
- [53] A. Donnachie and P.V. Landshoff, Phys. Lett. B 296 (1992) 227; L.A. Kondratyuk et al., Phys.Rev. C48 (1993) 2491; A.B. Kaidalov, L.A. Ponomarev and K.A. Ter-Martirosian Sov. J. Nucl. Phys. 44 (1986) 468; A.A. Sibirtsev, Sov. J. Nucl. Phys. 55 (1992) 145.
- [54] D. Lohse, J.W. Durso, K. Holinde and J. Speth, Nucl. Phys. A 516 (1990) 513; G. Janssen, B.C. Pearce, K. Holinde and J. Speth, Phys. Rev. D 52 (1995) 2690.
- [55] J-F. Germond and C. Wilkin, Nucl. Phys. A 518 (1990) 308.
- [56] T. Vetter, A. Engel, T. Biro and U. Mosel, Phys. Lett. B263 (1991) 153.
- [57] A. Sibirtsev, W. Cassing and C.M. Ko, Z. Phys. A 358 (1997) 101.

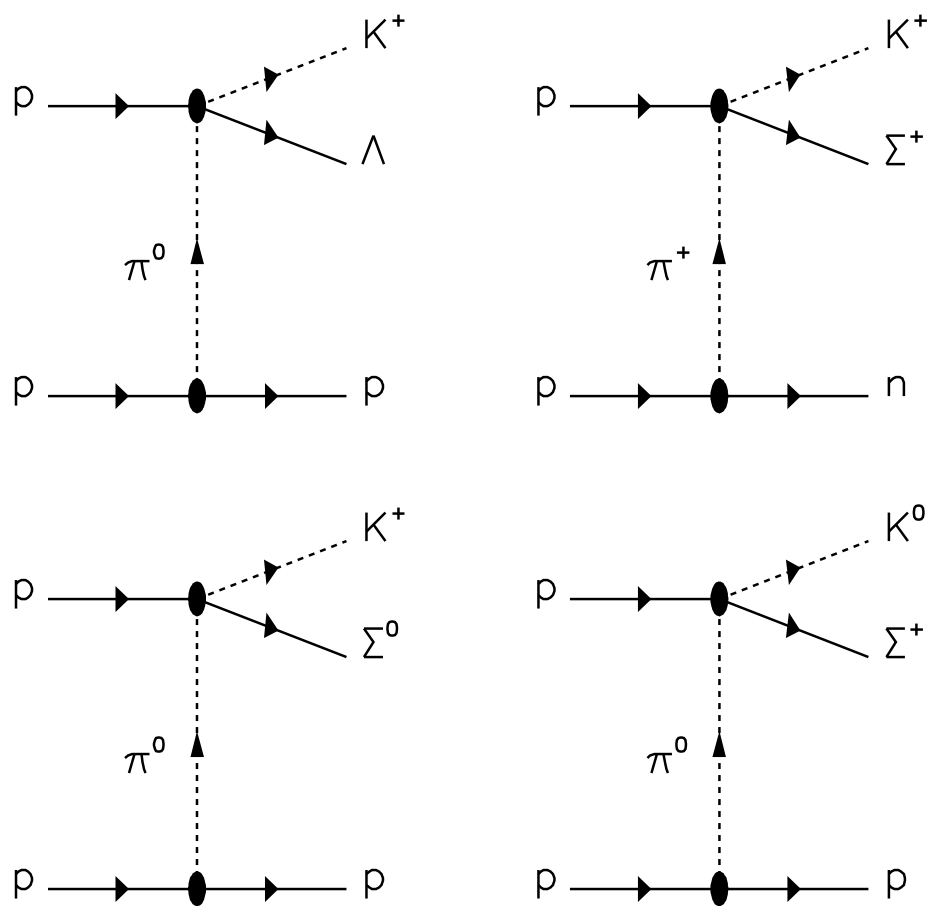


Figure 1: Pion exchange diagrams for $pp \rightarrow pYK$ reaction channels.

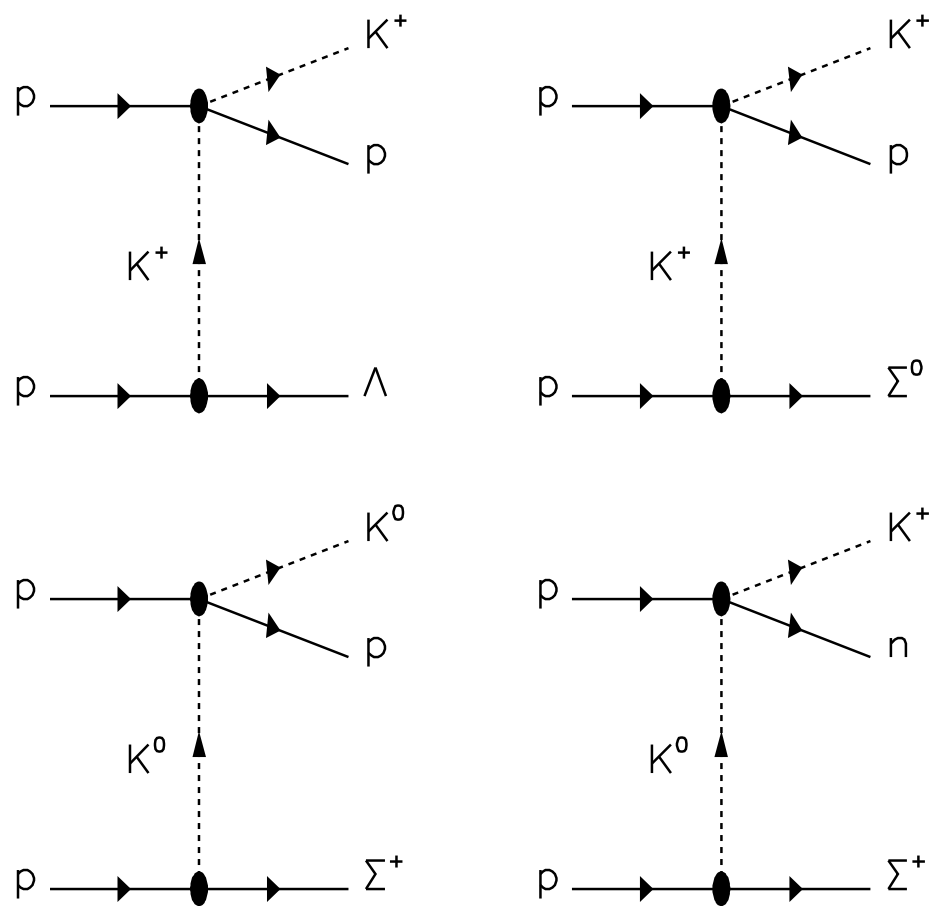


Figure 2: Kaon exchange diagrams for $pp \rightarrow pYK$ reaction channels.

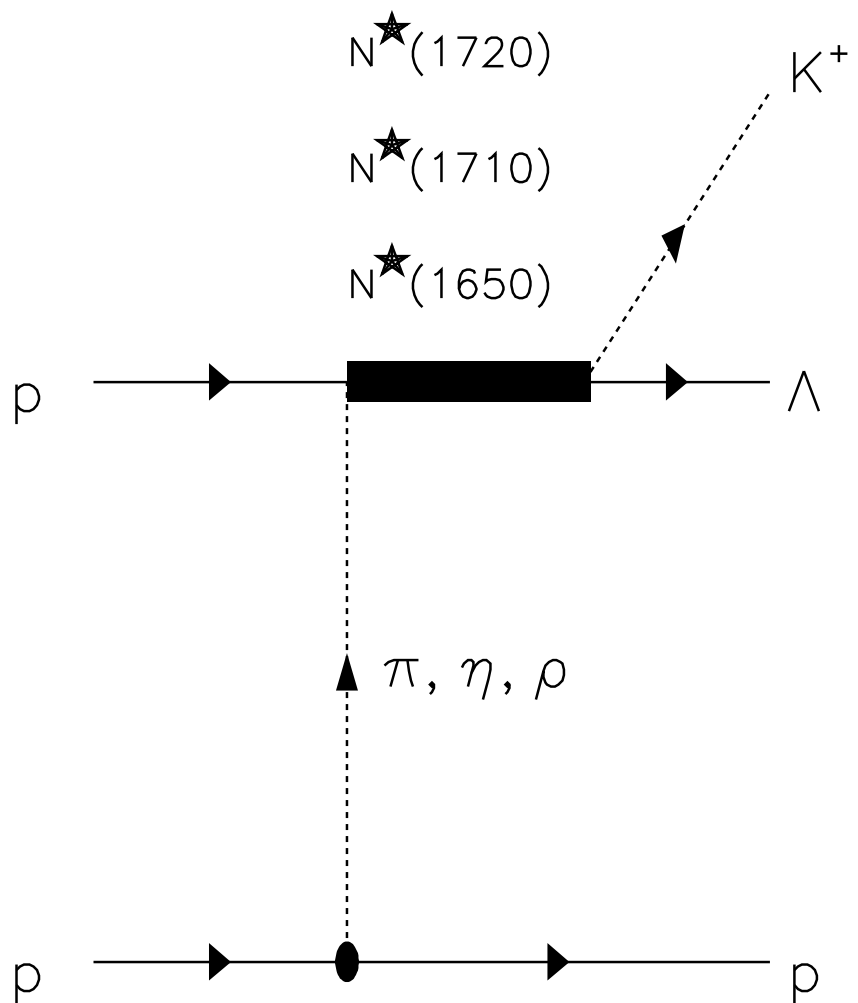


Figure 3: Meson exchange diagram for $pp \rightarrow p\Lambda K^+$ reaction in terms of the resonance model.

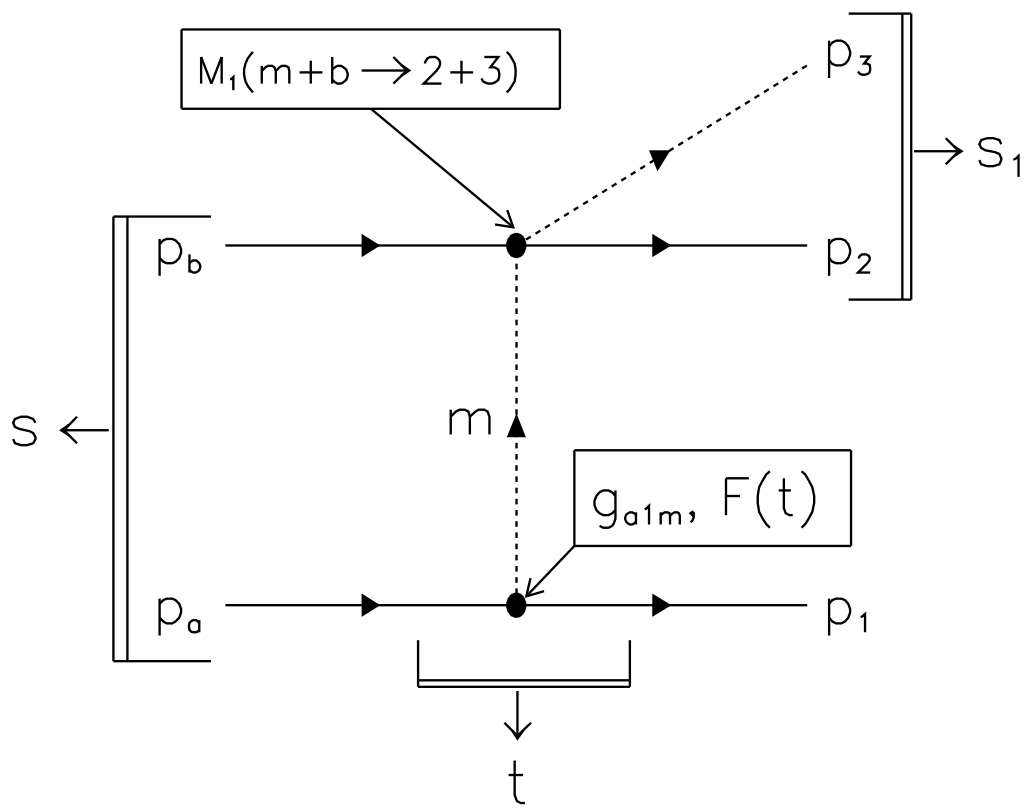


Figure 4: Feynman diagram for $a + b \rightarrow 1 + 2 + 3$ reaction.

$$\pi^- p \rightarrow \Lambda K^0$$

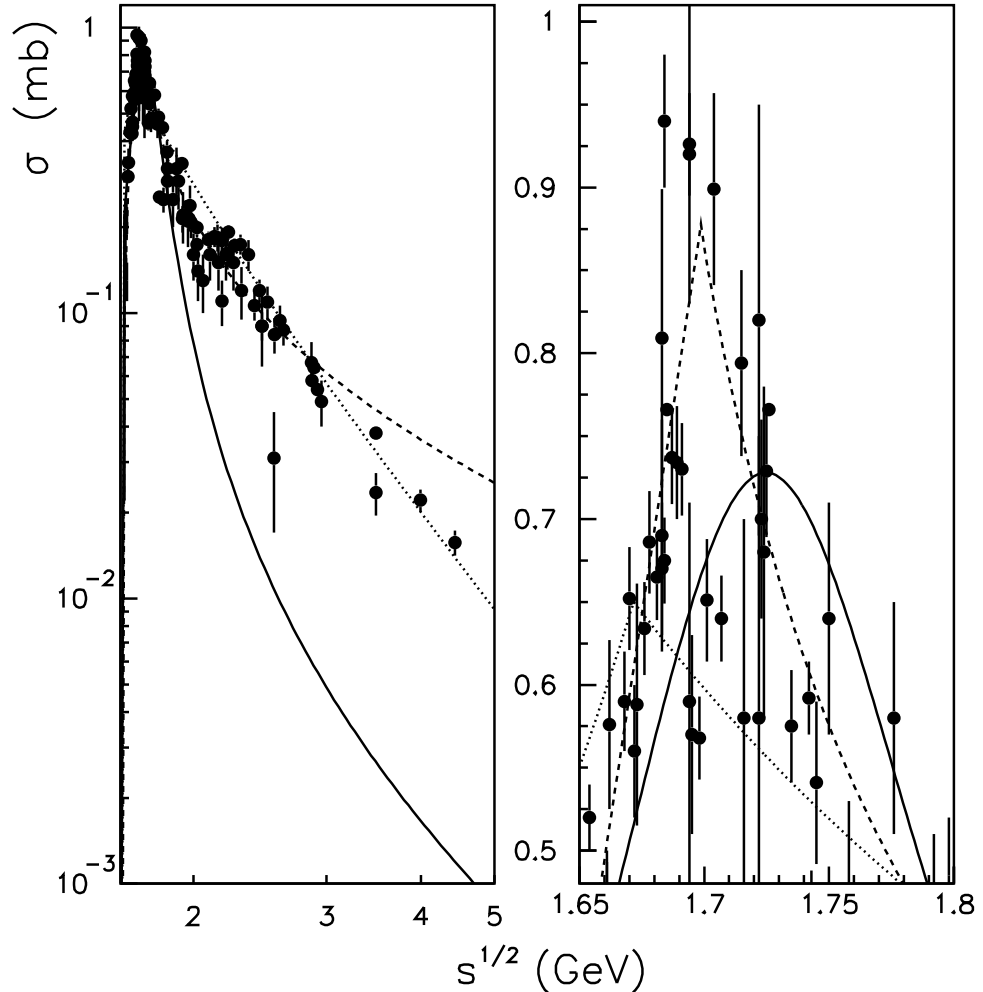


Figure 5: The cross section for the reaction $\pi^- p \rightarrow K^0 \Lambda$. Experimental points are from [16]. The lines show the parameterizations [25]-solid, [39]-dashed and [40]-dotted

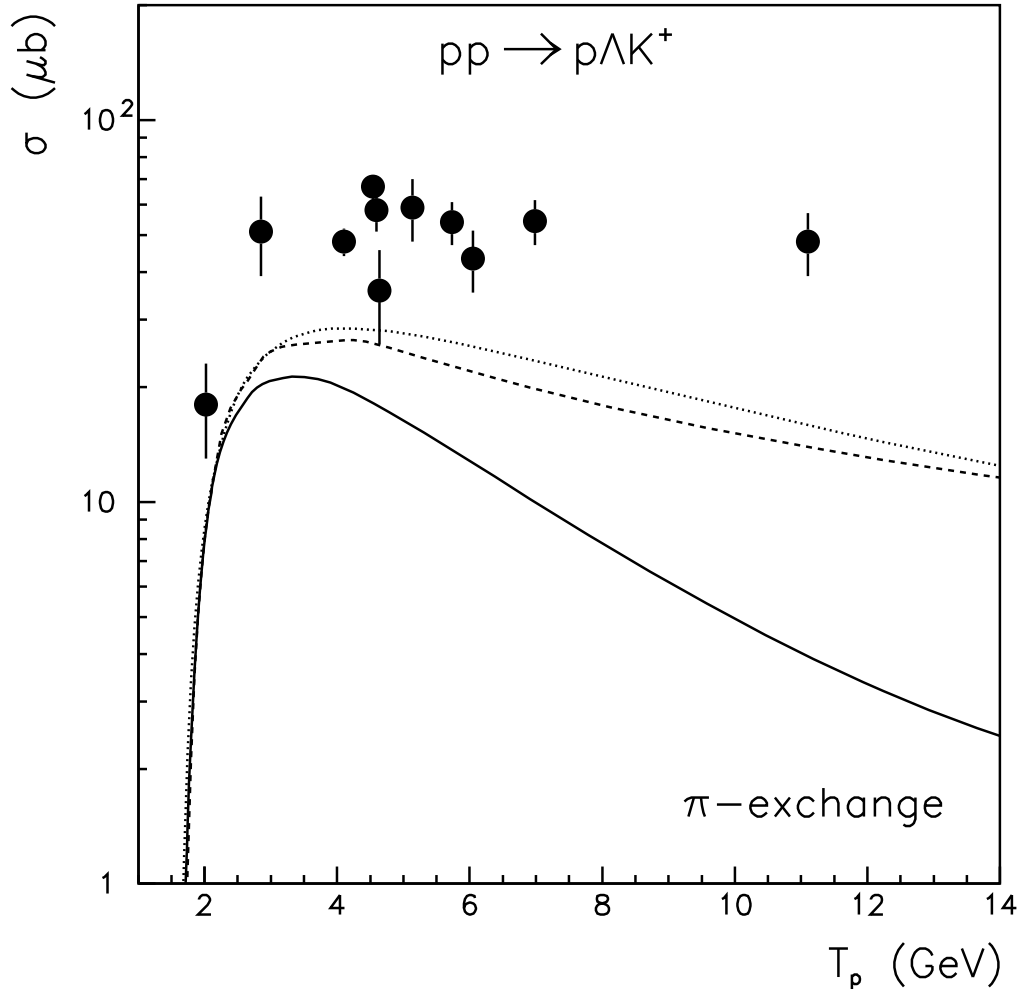


Figure 6: The cross section for the reaction $pp \rightarrow p\Lambda K^+$. Experimental points are from [16]. The lines show the results from the pion exchange model calculated with different πN amplitudes. The notations are the same as in Fig. 5.

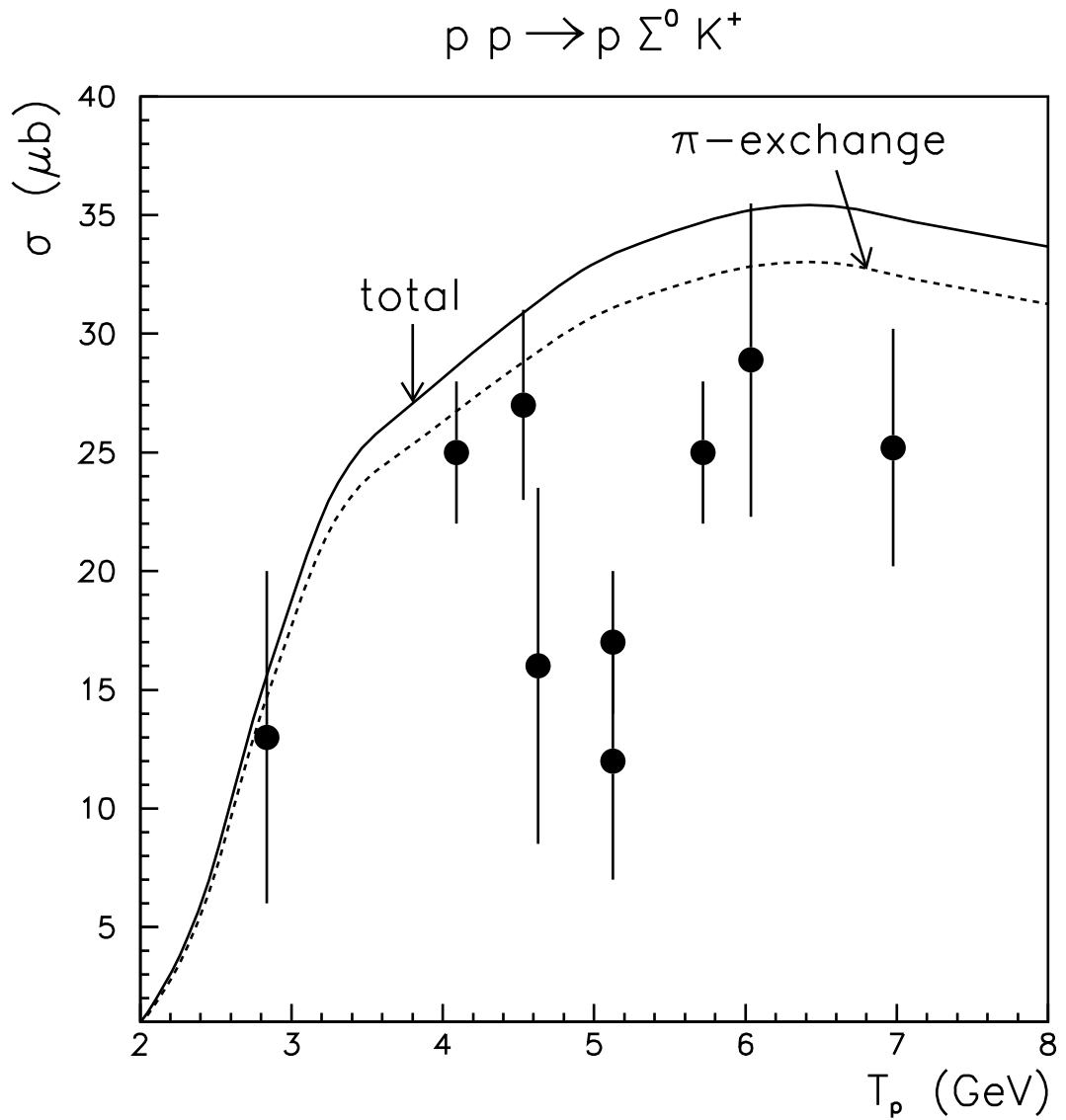


Figure 7: The cross section for the reaction $pp \rightarrow p\Sigma^0 K^+$. Experimental points are from [16]. The lines show the results from the boson exchange model. The solid line is the sum of the pion and kaon exchange; the dashed line shows pion exchange, only.

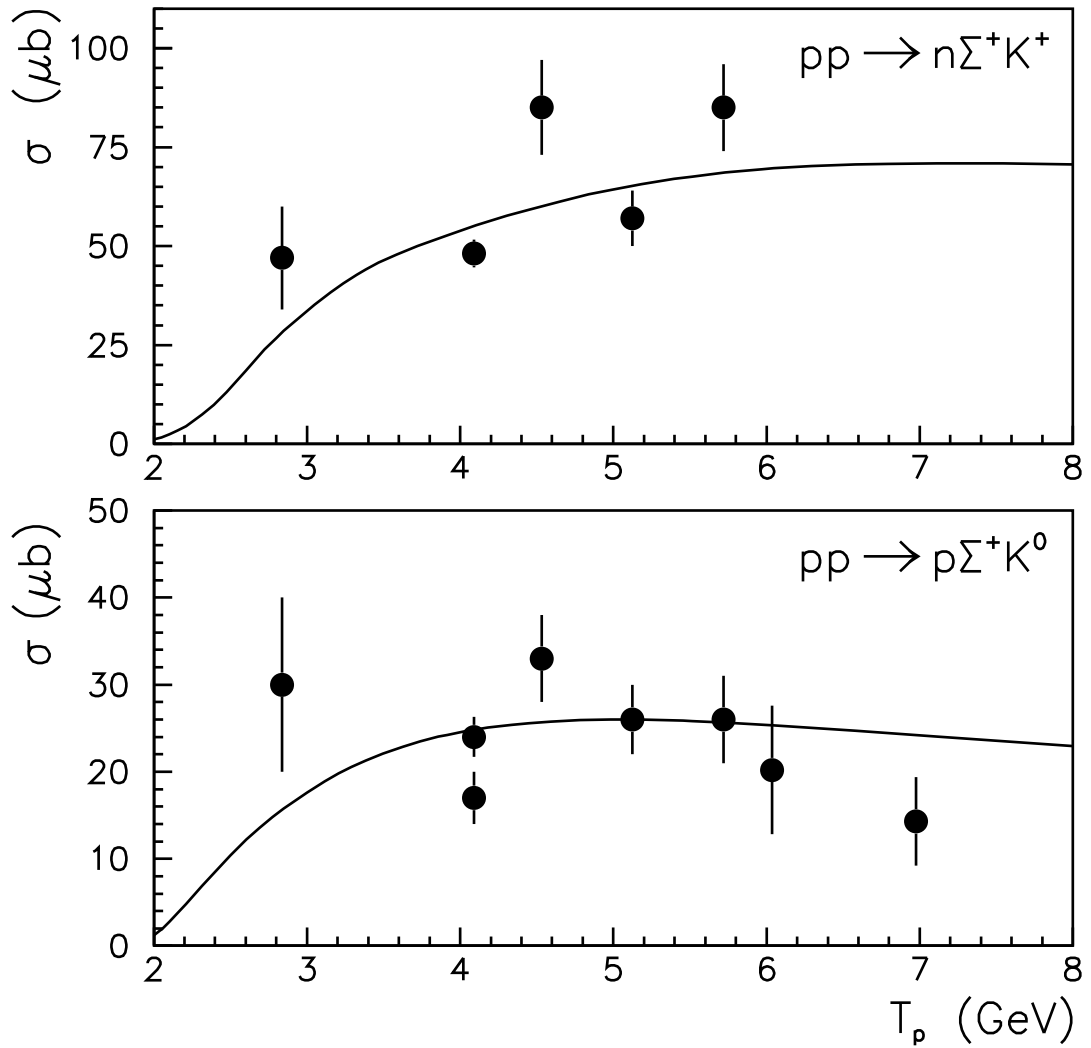


Figure 8: The cross section for the reactions $pp \rightarrow n\Sigma^+ K^+$ and $pp \rightarrow p\Sigma^+ K^0$ in comparison to the experimental data from [16]. The lines show the results from the boson exchange model.

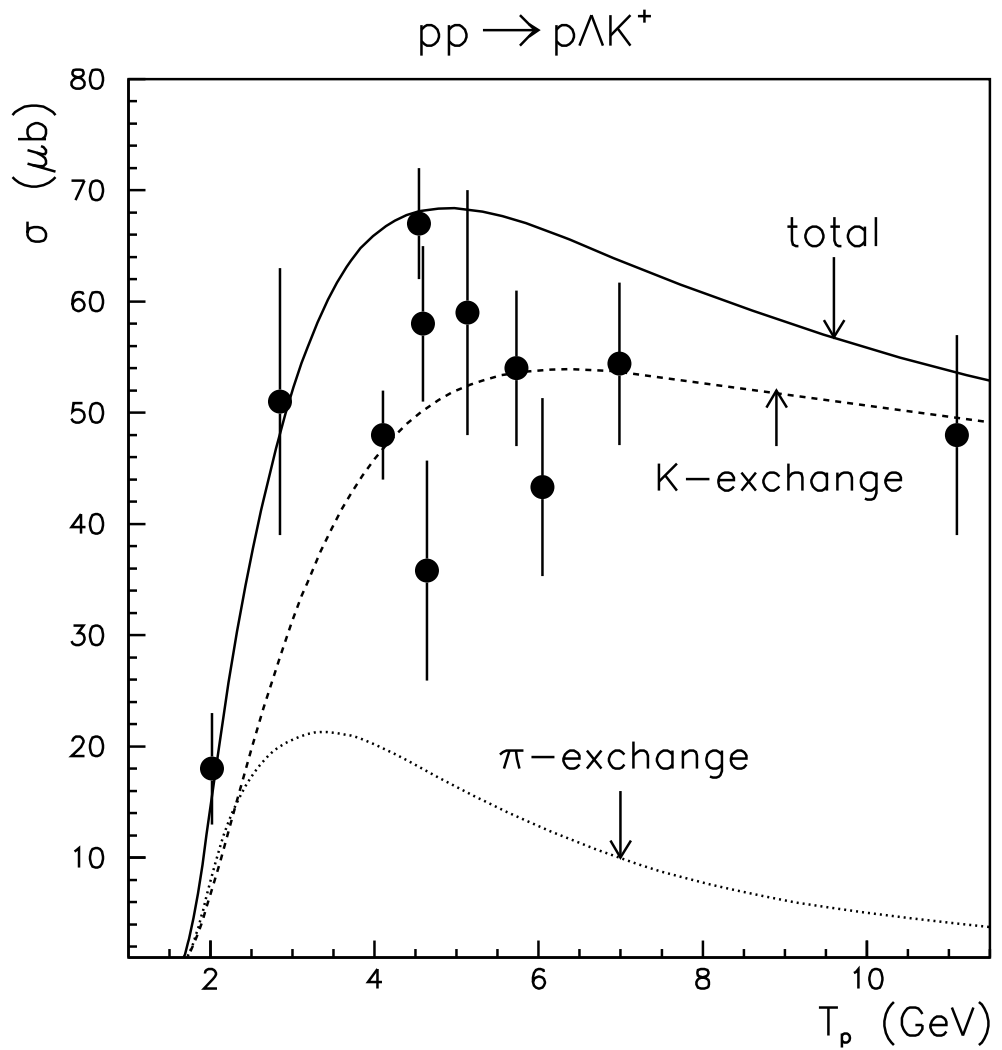


Figure 9: The cross section for the reaction $pp \rightarrow p\Lambda K^+$ in comparison with the experimental data from [16]. The lines show the results from the pion (dotted) and the kaon exchange model (dashed), while the solid line is the sum of both.

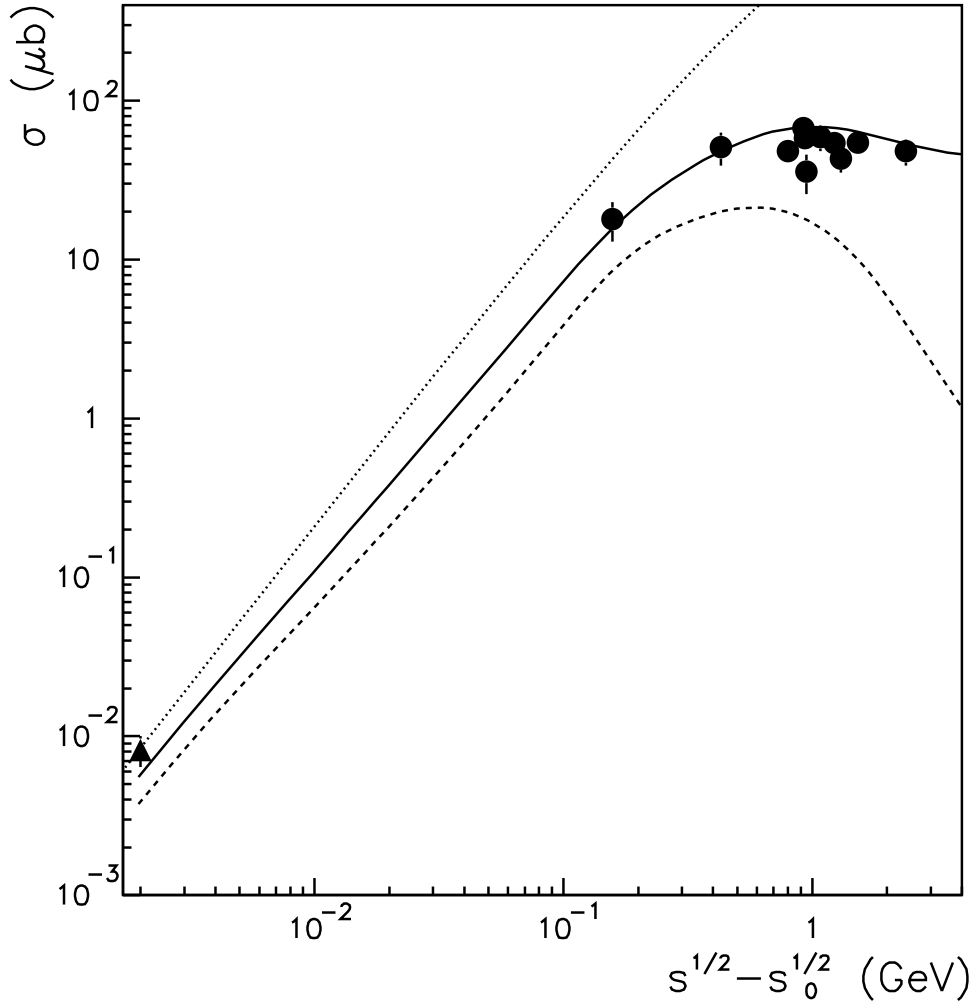
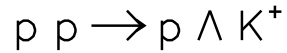


Figure 10: The $pp \rightarrow p\Lambda K^+$ cross section as function of the excess energy. Dots are the experimental data from [16] while the triangle is from [17]. The solid line shows our calculation with both pion and kaon exchanges, while the dashed indicates the result from one pion exchange only. The dotted line illustrates the phase space dependence of the production cross section.

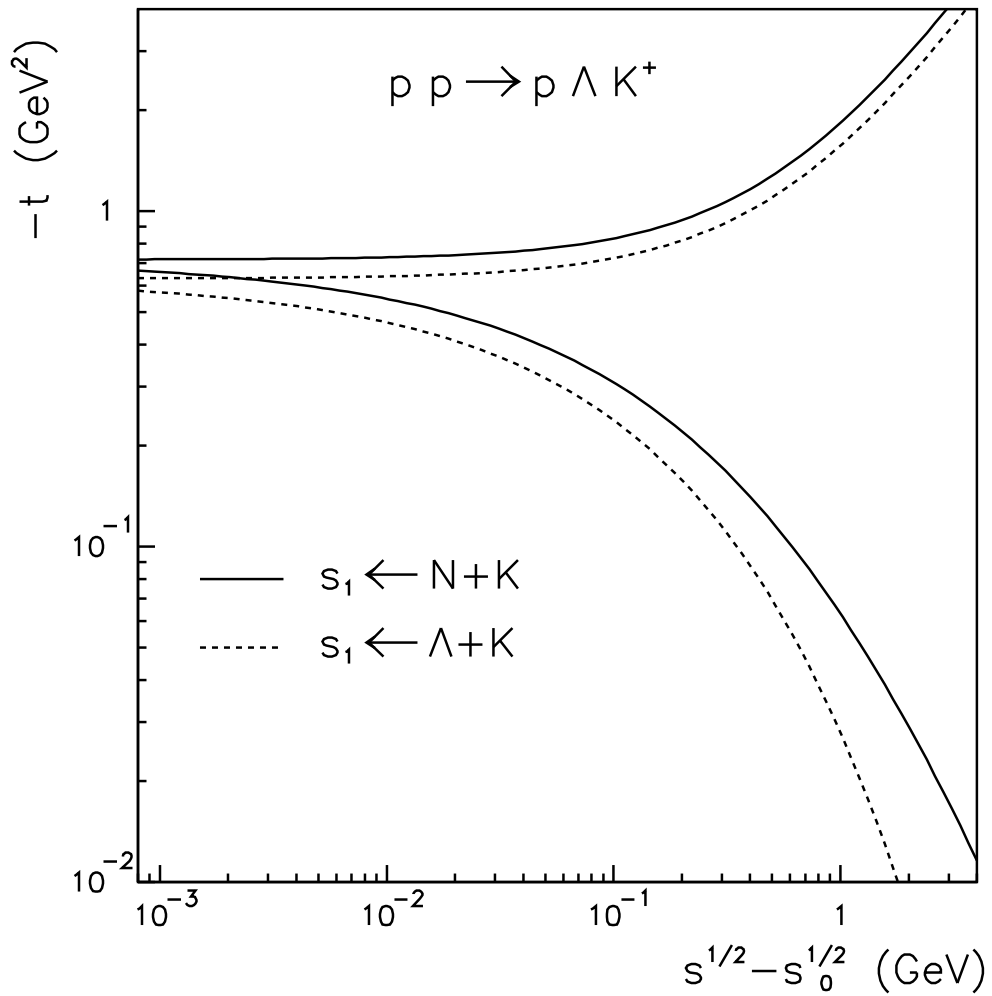


Figure 11: The momentum transfer as a function of the available energy above the $pp \rightarrow p\Lambda K^+$ reaction threshold. The lines indicate lower and upper limits. The solid lines stand for the one kaon exchange while the dashed are for the pion exchange model.

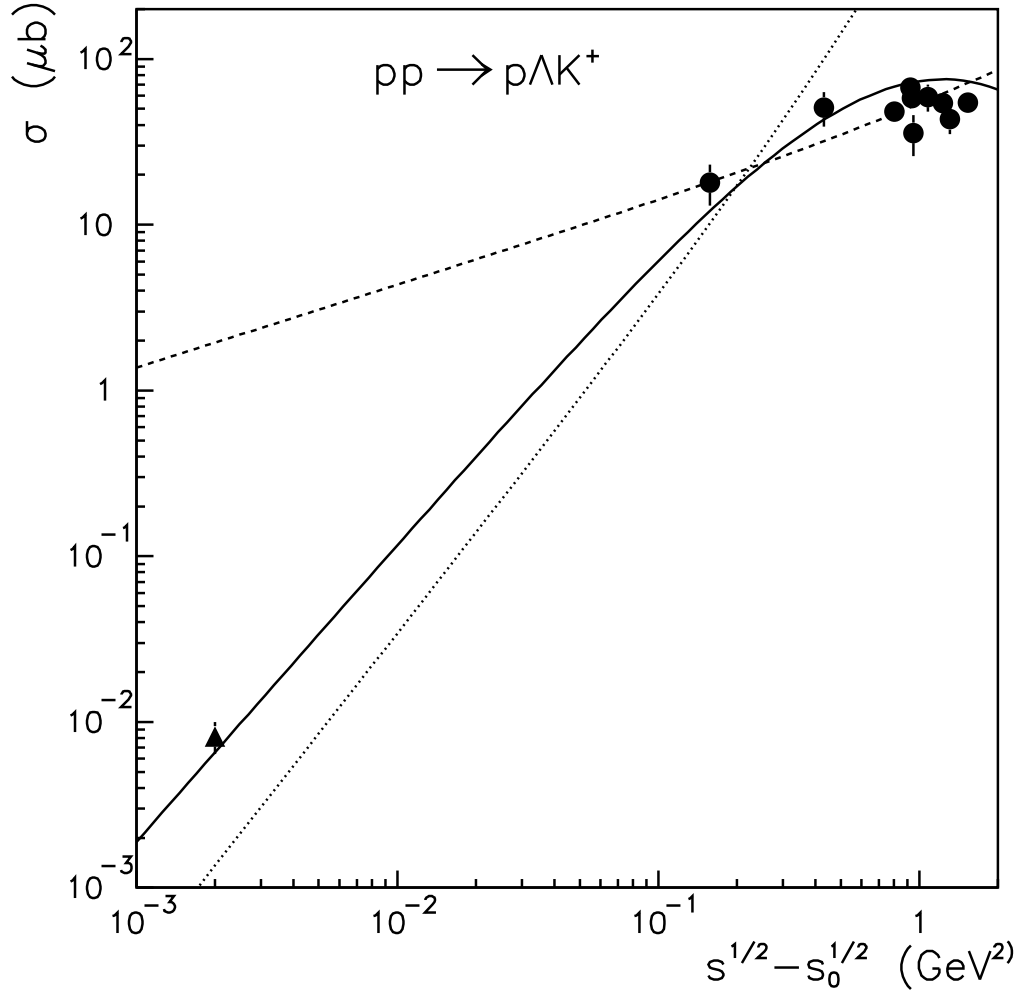


Figure 12: The cross section for the reaction $pp \rightarrow p\Lambda K^+$. The dots show the experimental data [16] while the triangle represents the result from COSY [17]. The solid line shows the results from the boson exchange model. The dashed line is the parameterization from Randrup and Ko (35) while the dotted line indicates the result from Schürmann and Zwermann (37).

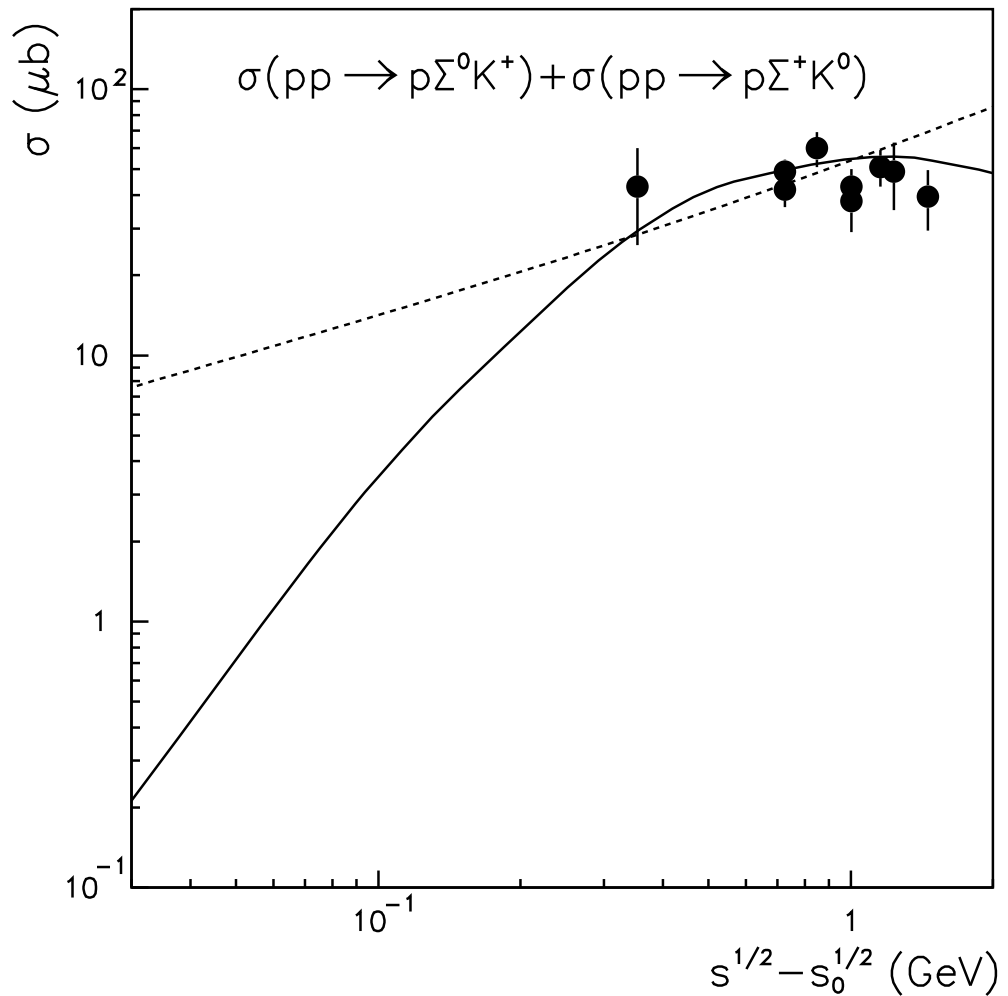


Figure 13: Sum of the $pp \rightarrow p\Sigma^0 K^+$ and $pp \rightarrow p\Sigma^+ K^0$ cross sections. The dots show the experimental data [16]. The solid line shows the result from the boson exchange model while the dashed line corresponds to the parameterization (35).

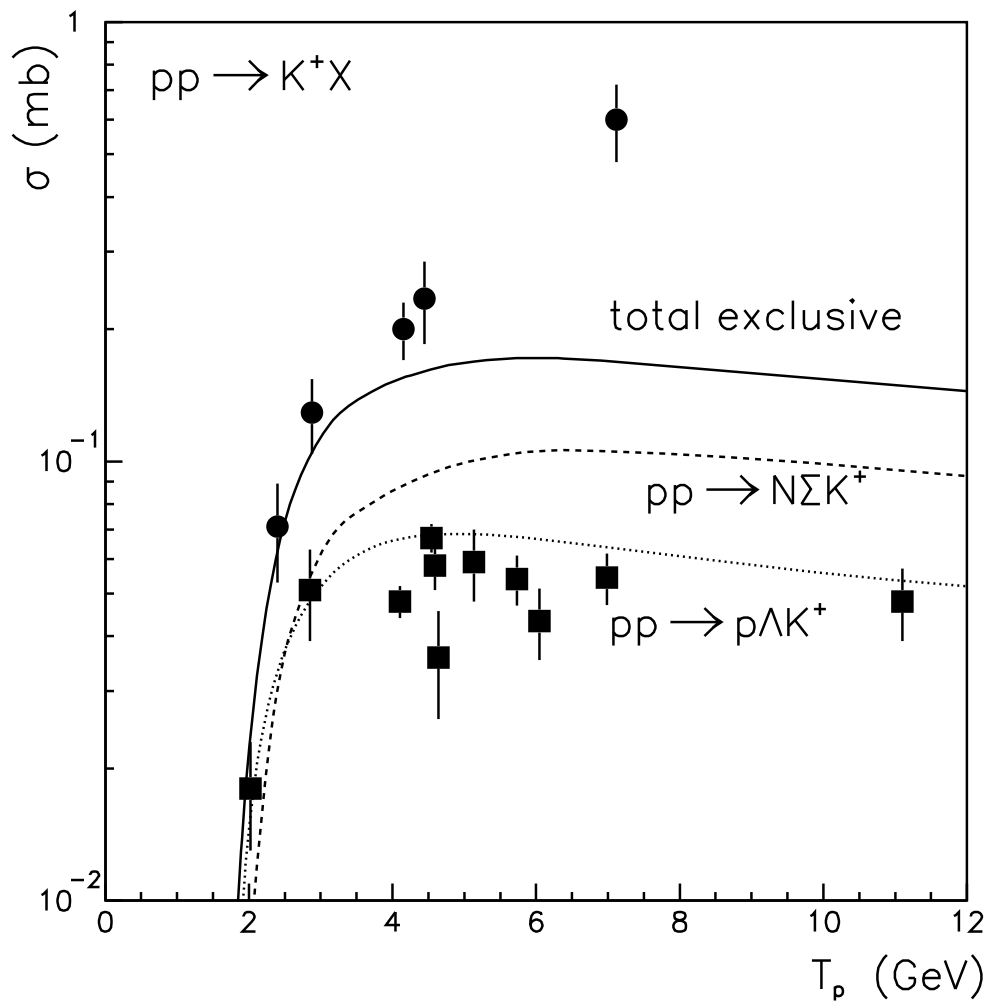


Figure 14: The cross section for inclusive K^+ production (full dots) and the reaction $pp \rightarrow p\Lambda K^+$ (squares). The lines show the contributions from the Λ channel - (dotted), Σ -(dashed) and the sum -(solid) calculated according to (34).